Geophys. J. Int. (2000) **140,** 37–50

Ground deformation in a viscoelastic medium composed of a layer overlying a half-space: a comparison between point and extended sources

Arnau Folch,[1] José Fernández,[2] John B. Rundle[3] and Joan Martí[1]

[1] *Institute of Earth Sciences 'Jaume Almera' (CSIC), c/Lluís Solé Sabarís s/n,* 08025 *Barcelona, Spain*
[2] *Instituto de Astronomía y Geodesia (CSIC-UCM), Facultad de C. Matemáticas, Ciudad Universitária,* 28040 *Madrid, Spain.*
E-mail: jft@iagmat1.mat.ucm.es
[3] *CIRES, University of Colorado at Boulder,* CO 80389, *USA*

Accepted 1999 July 30. Received 1999 July 30; in original form 1999 February 5

SUMMARY

We obtain and compare analytical and numerical solutions for ground displacement caused by an overpressurized magma chamber placed in a linear viscoelastic medium composed of a layer over a half-space. Di erent parameters such as size, depth and shape of the chamber, crustal rheology and topography are considered and discussed. Numerical solutions for an axisymmetric extended source are computed using a finite element method (FEM). Analytical solutions for a point source are obtained using the dislocation theory and the propagator matrix technique. In both cases, the elastic solutions are used together with the correspondence principle of linear viscoelasticity to obtain the solution in the Laplace transform domain. Viscoelastic solutions in the time domain are derived inverting the Laplace transform using the Prony series method. The di erences between the results allow us to constrain the applicability of the point source and the flat surface hypothesis, which are usually implicitly assumed when analytical solutions are derived. The e ect of the topography is also considered. The results obtained show that neglecting the topographic e ects may, in some cases, introduce an error greater than that implicit in the point-source hypothesis. Therefore, for an adequate modelling and interpretation of the time-dependent displacements, topography must be considered.

Key words: analytical model, ground deformation, magmatic intrusion, numerical model, viscoelasticity.

1 INTRODUCTION

The study of ground deformation inside active volcanic areas has been one of the most active topics in volcanology during the last decades. Mogi (1958) was the first to apply a point source of pressure in an elastic half-space to interpret ground deformation in areas of volcanic activity. The physical meaning generally ascribed to this model is that of a spherical buried magma chamber with a certain overpressure. Notwithstanding, this analytical model has been extensively and sometimes successfully employed, its intrinsic limitations called for more elaborated models. Thus, within the frame of the elastic models, McTigue (1987) derived an approximate analytical solution for the displacement and the stress fields that includes higher-order terms to represent the finite size of a spherical cavity. Davis (1986) developed solutions for ellipsoidal magma chambers. Bianchi *et al.* (1987) considered various spatial distributions of the elastic properties and McTigue & Stein (1984) and McTigue & Segall (1988) introduced the e ect of topography. Many increasingly more complex numerical models have been considered since the early work of Dieterich & Decker (1975). The numerical solutions of the elastic problem have allowed the computation of surface displacements and stresses considering several e ects such as extended sources, gravity, far-field stresses (e.g. Sartoris *et al.* 1990), structural discontinuities (e.g. De Natale & Pingue 1993; De Natale *et al.* 1997) and topography (e.g. Cayol & Cornet 1998; Williams & Wadge 1998). Considering the di erent models developed and the volcanic zones monitored, the existing bibliography on deformation modelling applied to volcanism, inflation processes in volcanic areas and the application of the models to the interpretation of data is so great that it is clearly not possible to include it all here. For an example, see the following and references therein: Rundle (1982a, 1983), Tilling

& Dvorak (1993), Delaney & McTigue (1994), Langbein *et al.* (1995), Rymer *et al.* (1995), Rymer (1996), De Natale & Pingue (1996), Dvorak & Dzurisin (1997), Bonafede & Mazzanti (1998), Delaney *et al.* (1998) and Fernández *et al.* (1999).

The solution of the mechanical problem considering an elastic rheology for the crust has allowed an explanation of the measured geodetic data in many volcanic areas with some success. However, in many cases the elastic models seem to be unable to reproduce the observed uplifts unless unrealistic overpressures are considered (e.g. Berrino *et al.* 1984). The problem of strain nuclei in an elastic layer overlying a viscoelastic half-space was investigated by Rundle (1978) to model the e ect of the asthenosphere. He assumed that the inelastic region (asthenosphere) had instantaneous elastic properties. Bonafede *et al.* (1986) pointed out that, in volcanic areas, the presence of incoherent materials and higher temperatures produces a lower e ective viscosity of the Earth's crust, which makes it necessary to consider its anelastic properties. They worked out analytical solutions for the displacements and associated stress fields induced by a pressure point source in a viscoelastic half-space and showed that the viscoelastic response may reproduce the observed uplifts with plausible overpressures. Several analytical models with anelastic properties have been proposed by di erent authors. Dragoni & Magnanensi (1989) derived the analytical solution for a spherical magma chamber surrounded by a viscoelastic shell and reproduced the order of magnitude of the ground uplift observed at Campi Flegrei. Bonafede (1990) rederived the analytical solution for a point-like spherical magma chamber and found a solution that provides a maximum uplift that is 1.8 times greater than the value obtained from Maruyama's strain nuclei given by Bonafede *et al.* (1986). Hofton *et al.* (1995) extended the work of Rundle (1980, 1981) and Fernández *et al.* (1996, 1998a) considering the existence of a gravitational field in a layered system with a viscoelastic half-space underlying an elastic layer with a dyke. Rundle (1980, 1982a, 1983), Fernández & Rundle (1994), Fernández *et al.* (1997) and Fernández *et al.* (1998b) derived the solution for a centre of expansion and a point mass in a multilayered medium, allowing both elastic and viscoelastic properties for the layers and bottom half-space.

Many of the models with anelastic properties considered so far are analytical and, generally, assume both a pressure point source and a flat surface. The advantage of these assumptions is that they allow one to obtain a relatively general and simple solution; however, they limit the applicability of the model. It is well known from the elastic case that the assimilation of the magma chamber with a point of dilatation implicitly assumes that the dimension of the body is small compared to its depth. However, the applicability of the point-source hypothesis to the viscoelastic problem has not yet been quantified. On the other hand, magma chambers characterized by depths comparable to their radii are not common, whilst inflation of shallow geothermal fields due to an increase in temperature or fluid pressure may be more common instances of inflating sources close to the ground surface. If these sources are spherical and the fluid is confined below the ground surface, the elastostatic solution outside the source volume is characterized by the same space pattern of overpressure sources (Bonafede 1990). In Bonafede (1991, 1995) the time-dependent inflation histories in two volcanic areas were interpreted in this way. These results made the necessity of obtaining solutions for extended sources and validating the point-like source assumption in all cases even clearer.

The objective of this paper is therefore to quantify the error produced in the viscoelastic solution by the point-source assumption. For this purpose, we compare analytical (point-source) and numerical (extended-source) solutions. The di erences between both methods are considered for di erent parameters such as size, shape and depth of the chamber, its overpressure and the type of relaxation. The influence of the topography is also investigated.

2 VISCOELASTIC SOLUTION

The objective is to determine the surface deformation field for a general axisymmetric problem (see Fig. 1) in which an ellipsoidal magma chamber with an overpressure ΔP and semi-axes a and b is buried at depth h_c below the Earth's surface. The chamber is characterized by its size-to-depth ratio, $\varepsilon \equiv b/h_c (0 < \varepsilon < 1)$. The e ect of the topography is represented by a volcano with height H and average slope of the flanks α. The rheological behaviour of the crust is represented by a homogeneous flat layer with thickness d overlying a homogeneous half-space. Both the layer and the half-space can have their own independent rheological properties.

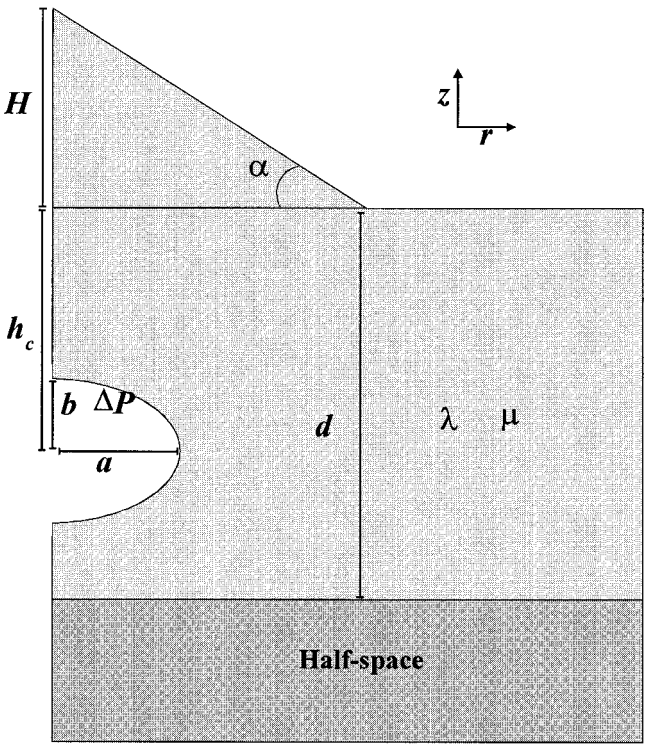

Figure 1. Schematic illustration of the problem. An ellipsoidal magma chamber with semi-axes a and b is buried at depth h_c below the surface of the Earth. The ratio size/depth is $\varepsilon \equiv b/h_c$. A volcano with height H and average slope of the flanks α is also considered in the general case (when $\alpha = 0$, i.e. $H = 0$, the e ect of the topography is neglected). The chamber has an overpressure ΔP. The crust is represented by a homogeneous flat layer with thickness d and Lamé parameters λ and μ. The layer overlies a homogeneous half-space, and both can have their own rheological properties; that is, they can behave elastically or can relieve imposed stresses by flowing in response.

Several linear and non-linear viscoelastic rheological models can be applied to deformation problems (e.g. Christensen 1971; Nur & Mavko 1974; Barker 1976; Melosh 1976; Rundle 1976, 1978, 1982b; Peltier 1982; Melosh & Raefsky 1983; Amelung & Wolf 1994; Wolf 1984; Körnig & Müller 1989; Ding & Shen 1991; Fernández *et al.* 1996, 1998a; Yu *et al.* 1996, 1999; Pollitz 1997; Vermeersen *et al.* 1996; Deng *et al.* 1998). It will be assumed throughout the present work that the inelastic region does possess instantaneous elastic properties. We will consider for the inelastic regime materials that have linear constitutive laws as in Rundle (1978, 1982b). Non-linear rheologies present greater mathematical di culties and they are not considered in this work.

The flow properties of the medium are of interest also. Nur & Mavko (1974) used a standard linear solid (SLS) rheology, while Peltier (1974), Barker (1976), Rundle (1976, 1978), Rundle & Jackson (1977a,b,c), Peltier (1982), Amelung & Wolf (1984), Wolf (1985), Ding & Shen (1991), Pollitz (1997) and Vermeersen *et al.* (1997) used a Maxwell viscoelastic fluid. Rundle (1982b) and Bonafede *et al.* (1986) used SLS and Maxwell rheologies. These two rheologies di er in that the former behaves as an elastic solid in the limit of both high and low frequencies, whereas the latter is an elastic solid at high frequencies and a Newtonian fluid at low frequencies.

The results obtained by Bonafede *et al.* (1986) show that the e ect of viscoelasticity is a long-term amplification of the sudden initial elastic deformation. This e ect is, however, di erent according to the kind of source considered. In the centre of the dilation model, the maximum amplifications are obtained for a Maxwell solid rheology. In this case, the final viscoelastic deformation is 20 per cent larger than the initial elastic one. Stress is completely relaxed in the long term. In the pressure source model, with an SLS rheology, the viscoelastic amplification is larger than in the centre of the dilation model. Bonafede *et al.* (1986) considered that both models are inadequate to represent the deformation in volcanic areas, although the introduction of viscoelasticity helps to obtain less unreasonable values for the pressure change responsible for the ground displacements. On the other hand, in the pressure source model with a Maxwell solid rheology, they found that the behaviour of the solution is di erent. In fact, the viscoelastic displacement has no finite limit for $t \to \infty$, but grows indefinitely in time. The geophysical observable that has to be explained by such a model is thus the uplift rate, rather than the total uplift. With the introduction of viscoelasticity, the required value of the pressure applied to the source surface is reduced by a factor of 10 or more, so that only a few tens of bars may be enough to produce the uplift.

For a linear viscoelastic material, the solution of the governing equations can be obtained from the elastic solution employing the correspondence principle (Fung 1965; Christensen 1971). The analytical solution of the elastic problem is obtained using the dislocation theory and the propagator matrix technique (an extensive description of this method can be found in Rundle 1980, 1982a, 1983; Fernández *et al.* 1997). The numerical solution is obtained using a finite element method. Boundary conditions are summarized in Fig. 2. The upper boundary is traction free and represents the surface of the Earth. Displacements are fixed to zero at the bottom and lateral boundaries. These boundaries are located a long way

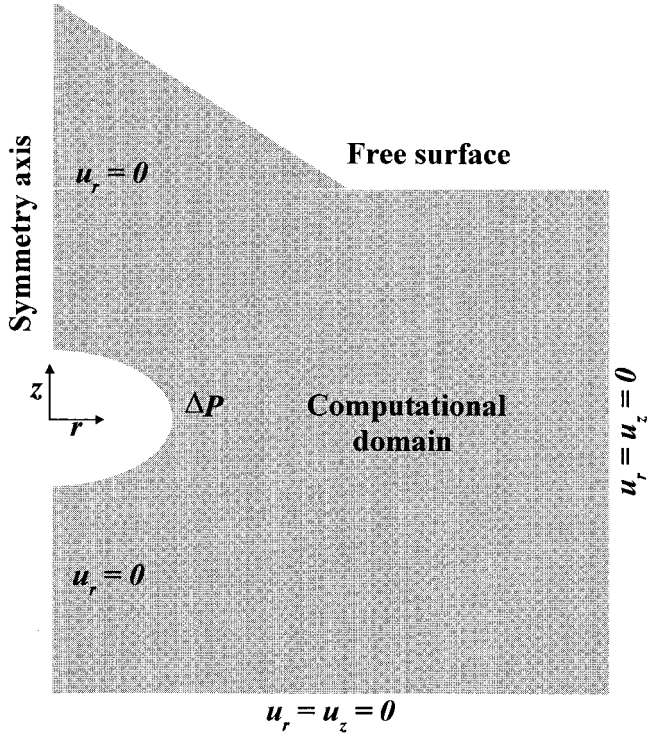

Figure 2. Schematic cartoon showing the boundary conditions used in the numerical computations. The axis of symmetry is located at $r = 0$. The radial displacement at the symmetry axis is set to zero. The chamber has an overpressure ΔP. The surface of the Earth is a free surface, whereas the basal and lateral boundaries are fixed. These boundaries are located far away from the chamber in order to avoid the influence of the boundary conditions on the solution.

from the magma chamber in order that they do not measurably a ect the results. The finite element meshes used in computations consist of quadratic bilinear Lagrangian elements (nine nodes per element) and contain an average of 10 000 nodal points. The finite element source code has been written by the authors and tested using several benchmark problems.

In the computation of the Green functions considered in the following section we allow the layer to be elastic or viscoelastic. The bottom half-space is always considered to be viscoelastic. As there appears to be no particular reason for requiring the Lamé constant λ to be viscoelastic (Rundle 1978, 1982b), we can keep it constant. Also, the fact that we can choose the rheology of λ and μ independently is easily shown (Christensen 1971; Rundle 1978). Finally, we can select rheologies as described by Peltier (1974), who also had a Maxwell μ but had λ as a standard linear solid.

In all cases, the general procedure to find the viscoelastic solution is to replace the elastic Lamé parameters λ and μ by some functions $\tilde{\lambda}(s)$ and $\tilde{\mu}(s)$, where s is the Laplace transform variable. The resulting expression is the Laplace transform of the viscoelastic solution, which must be inverted in order to obtain the viscoelastic solution in the time domain.

The specific values of $\tilde{\lambda}(s)$ and $\tilde{\mu}(s)$ depend on the rheology considered. It is well known that the physical meaning of λ is not as clear as Young's modulus, the bulk modulus, the shear modulus and Poisson's ratio. It arises more from the convenience of writing the normal stresses in terms of the normal

strains (see e.g. Davis & Selvadurai 1996). λ is required to be non-zero as time tends toward infinity. Various kinds of rheologies are possible. For example, if the crust is infiltrated by pore fluids so that volumetric changes are possible in response to mean stress, the shear modulus would be elastic, while the bulk modulus would relax (see e.g. Rundle 1982c; Berryman 1992). This kind of crustal rheology can be modelled by using an elastic shear modulus and an SLS bulk modulus. On the other hand, shear relaxation of crustal material is also possible via a 'melt-squirt' mechanism (e.g. Mavko & Nur 1975). In the latter case, the shear modulus has an SLS behaviour, while the bulk modulus is purely elastic. Many other rheological models are possible as well, for both the crust and the asthenosphere. The only real constraint upon the behaviour of $\tilde{\lambda}(s)$ or $\tilde{\mu}(s)$ at any depth is that the time-dependent bulk modulus can never be zero, otherwise the material could in principle compress to zero volume. Since in this paper our goal is to examine the physical behaviour of a number of possible models arising from di erences in rheology, we therefore consider three di erent possibilities for the rheology of $\tilde{\lambda}(s)$ and $\tilde{\mu}(s)$ (Rundle 1982b). We also compare di erences in results for point and extended sources.

The first possibility is denoted by Relaxation 1, which we call 'asthenospheric relaxation', in which the crust deforms viscoelastically with respect to the shear stresses as a Maxwell body but behaves elastically with respect to the normal stresses. In this case, one has

$$\tilde{\lambda}(s) = \lambda, \tag{1a}$$

$$\tilde{\mu}(s) = \mu\tau/(s\tau + 2), \tag{1b}$$

$$\tau = 2\eta/\mu, \tag{1c}$$

where λ and μ are the elastic Lamé parameters, τ is the characteristic time and η is the viscosity. Note that in the asthenospheric relaxation, only the Lamé parameter μ is replaced by the function $\tilde{\mu}(s)$, while λ is left as in the elastic case.

The second option is called Relaxation 2, in which the crust deforms viscoelastically as a Maxwell fluid with respect to both the shear and the normal stresses but the Poisson's coe cient is kept constant. In this case

$$\tilde{\lambda}(s) = \lambda\tau/(s\tau + 2), \tag{2a}$$

$$\tilde{\mu}(s) = \mu\tau/(s\tau + 2). \tag{2b}$$

In the third option, denoted by Relaxation 3, the crust deforms viscoelastically with respect to both the shear and the normal stresses but the bulk modulus is kept constant. In particular, the shear modulus relaxes as a Maxwell fluid; however, λ relaxes as a standard linear solid, so that the bulk modulus remains constant (see, e.g. Peltier 1998 p. 621). Then,

$$\tilde{\mu}(s) = \mu\tau/(s\tau + 2), \tag{3a}$$

$$\tilde{\lambda}(s) = \lambda + 2\mu/3 - 2\tilde{\mu}(s)/3. \tag{3b}$$

The specific method used to perform the inversion is the Prony series method (see: Schapery 1961; Cost 1964; Rundle 1982b). In this method, an arbitrary scalar function $f(t)$ is approximated by a series of decaying exponentials,

$$f(t) \cong \sum_{i=1}^{N} A_i\tau_i(1 - e^{-t/\tau_i}), \tag{4}$$

where $\cong$ means 'approximately equal to in the least square sense', τ_i is a set of N known relaxation times and the A_i are the set of unknown constants that can be determined by the least-squares method. Rundle (1982b) showed that good results for the inversion can be obtained by choosing the set of relaxation times as

$$\{\tau_i\} = \{0.5\tau, \tau, 5\tau, 10\tau, 50\tau, 100\tau\} \text{(i.e. } N = 6), \tag{5}$$

where τ is the relaxation time defined in (1c). If the Laplace transform is applied to (4), one obtains

$$s\tilde{f}(s) = \sum_{i=1}^{N} A_i\tau_i \frac{1}{1 + s\tau_i}. \tag{6}$$

The above expression must be verified for any value of s and, in particular, for the N values $s_j = 1/\tau_j$. Then, providing that the Laplace transform $\tilde{f}(s)$ is known (using either analytical or numerical methods), expression (6) can be transformed into an algebraic system of N equations with N unknowns that determine the interpolation constants A_i:

$$\mathbf{F} = \mathbf{K} \cdot \mathbf{a}, \tag{7}$$

where

$$\mathbf{K}_{ij} = \frac{\tau_i\tau_j}{\tau_i + \tau_j}, \tag{8a}$$

$$\mathbf{F}_i = \frac{1}{\tau_i}\hat{f}\left(\frac{1}{\tau_i}\right), \tag{8b}$$

$$\mathbf{a} = \begin{pmatrix} A_1 \\ \vdots \\ A_N \end{pmatrix}. \tag{8c}$$

The resolution of system (7) determines the constants A_i and, in consequence, determines the inverse Laplace transform (4). From a numerical point of view, a combination of the correspondence principle and the Prony series method provides an e cient, extremely cost-e ective method to solve the viscoelastic problem. One must proceed as follows.

(i) Solve the elastic problem as usual to obtain the solution at $t = 0$.

(ii) Solve N additional elastic problems (one for each value of τ_i), replacing the Lamé parameters λ and μ by $\tilde{\lambda}(1/\tau_i)$ and $\tilde{\mu}(1/\tau_i)$ respectively. Both the Dirichlet and the Neumann boundary conditions must also be Laplace-transformed.

(iii) Use (7) to obtain the coe cients A_i at each nodal point and (4) to determine the viscoelastic solution.

3 COMPARISON BETWEEN ANALYTICAL AND NUMERICAL SOLUTIONS

The surface displacements produced by the viscoelastic response depend on several parameters such as size, depth and shape of the chamber, the chamber overpressure, the type of relaxation and the topography. Di erent tests have been performed in order to evaluate the influence of these parameters on the viscoelastic solution as well as the validity of the point-source hypothesis. In each test, all the parameters except the one under study are fixed in order to analyse the influence of this

parameter on the solution. For all cases, Young's modulus is 75 GPa and the Poisson's ratio is 0.25 (both Lamé parameters are then 30 GPa). The rest of the values employed in the tests are summarized in Table 1. Viscoelastic solutions are given in terms of the characteristic time defined in (1c), so that some value for the crust's viscosity must necessarily be assumed for practical applications.

Test 1 and Test 2 consider the influence of the size and the depth of the chamber on the viscoelastic solution. In both cases, the chamber is assumed to be spherical with an overpressure of 10 MPa. The viscoelastic relaxation of the layer and the half-space is Relaxation 2. Fig. 3 shows the vertical and radial surface displacements for chambers located at 3 km depth and with radii of 0.5, 1 and 2 km, respectively. Fig. 4 shows the same results for chambers with radii of 1 km but located at depths of 3, 6 and 9 km. It is seen from these figures how, as in the elastic case (e.g. Dieterich & Decker 1975), the analytical and numerical solutions tend to converge for small radius/depth ratios (small ε-values) but, in contrast, when ε increases appreciable discrepancies produced by the point-source hypothesis appear. When ε is small, the di erences are below or within the centimetre range, being 5–20 per cent of the maximum displacement (in both radial and vertical displacements). However, for higher values of ε, the discrepancies are greater than 30 per cent and can have, in some cases (see Fig. 3c), an absolute value in the range of 1 m. When ε is small, the absolute value of the di erence between the two solutions is very similar to that in the elastic case ($t = 0$), but when ε approaches 1 this absolute value increases with time. However, we observe that, whatever the value of ε, the relative error decreases for long τ values, despite the fact that the absolute di erence between the two solutions may increase. This fact is reflected in Fig. 5, which shows the relative vertical error at the point of maximum uplift ($r = 0$) as a function of time using the same assumptions as for Fig. 3(b).

Test 3 considers the e ect of the shape of the chamber. Fig. 6 shows numerical results for ellipsoidal chambers with minor axis $b = 0.5$ km and major axis $a = 0.5$, 1, 1.5 and 2 km, the corresponding eccentricities being 0, 0.86, 0.94 and 0.96 respectively. In all cases, the chamber is at 3 km depth and has an overpressure of 10 MPa. In order to test the influence of the shape of the chamber, analytical solutions are also obtained but considering spherical sources with an equal volume (the equivalent radii are 0.5, 0.8, 1.04 and 1.26 respectively). Note that for all cases the value of ε is always the same ($\varepsilon = 0.16$). For spherical chambers, analytical and numerical solutions give approximately the same result since ε is small. However, important discrepancies are observed when the eccentricity increases. Fig. 6 shows that di erences as higher as 100 per cent can appear when the eccentricity of the chamber is neglected.

In test 4, we analysed the influence of the overpressure. It is well known that, in the elastic case, the vertical displacement at the surface is proportional to ΔP (e.g. McTigue 1987). This result is also true for the viscoelastic solution due to the linearity of the Laplace transform and has also been checked with both the numerical and the analytical methods.

The influence of the relaxation type is analysed in Test 5. The most illustrative results for this test are shown in Fig. 7. All the results were obtained for a chamber located at 3 km depth with an overpressure of 10 MPa, but considering di erent types of relaxation for the layer and the bottom half-space (see Table 1). We have observed that, in general, the di erences between analytical and numerical solutions are not

Table 1. Values of the parameters used in the tests. Poisson's ratio is 0.25 and Young's modulus is 75 GPa. The Lamé parameters are 30 GPa. The meaning of each parameter is illustrated in Fig. 1.

	h_c (km)	a (km)	b (km)	$\varepsilon = b/h_c$	ΔP (MPa)	Layer	Half-space	α (°)
Test 1	3	0.5	0.5	0.16	10	Relaxation 2	Relaxation 2	0
(size)	3	1	1	0.33	10	Relaxation 2	Relaxation 2	0
	3	2	2	0.66	10	Relaxation 2	Relaxation 2	0
Test 2	3	1	1	0.33	10	Relaxation 2	Relaxation 2	0
(depth)	6	1	1	0.16	10	Relaxation 2	Relaxation 2	0
	9	1	1	0.11	10	Relaxation 2	Relaxation 2	0
Test 3	3	0.5	0.5	0.16	10	Relaxation 2	Relaxation 2	0
(shape)	3	1	0.5	0.16	10	Relaxation 2	Relaxation 2	0
	3	1.5	0.5	0.16	10	Relaxation 2	Relaxation 2	0
	3	2	0.5	0.16	10	Relaxation 2	Relaxation 2	0
Test 4	3	1	1	0.33	5	Relaxation 2	Relaxation 2	0
(overpressure)	3	1	1	0.33	10	Relaxation 2	Relaxation 2	0
	3	1	1	0.33	15	Relaxation 2	Relaxation 2	0
Test 5*	3	1	1	0.33	10	Relaxation 2	Relaxation 1	0
(relaxation)	3	1	1	0.33	10	Elastic	Relaxation 2	0
	3	1	1	0.33	10	Relaxation 3	Relaxation 2	0
Test 6†	2	1	1	0.5	10	Relaxation 2	Relaxation 2	0
(topography)	2	1	1	0.5	10	Relaxation 2	Relaxation 2	15
	2	1	1	0.5	10	Relaxation 2	Relaxation 2	20
	2	1	1	0.5	10	Relaxation 2	Relaxation 2	30

*In this case $d = 10$ km.
†The height of the volcano is $H = 0$, 1340, 1820 and 2886 m, respectively.

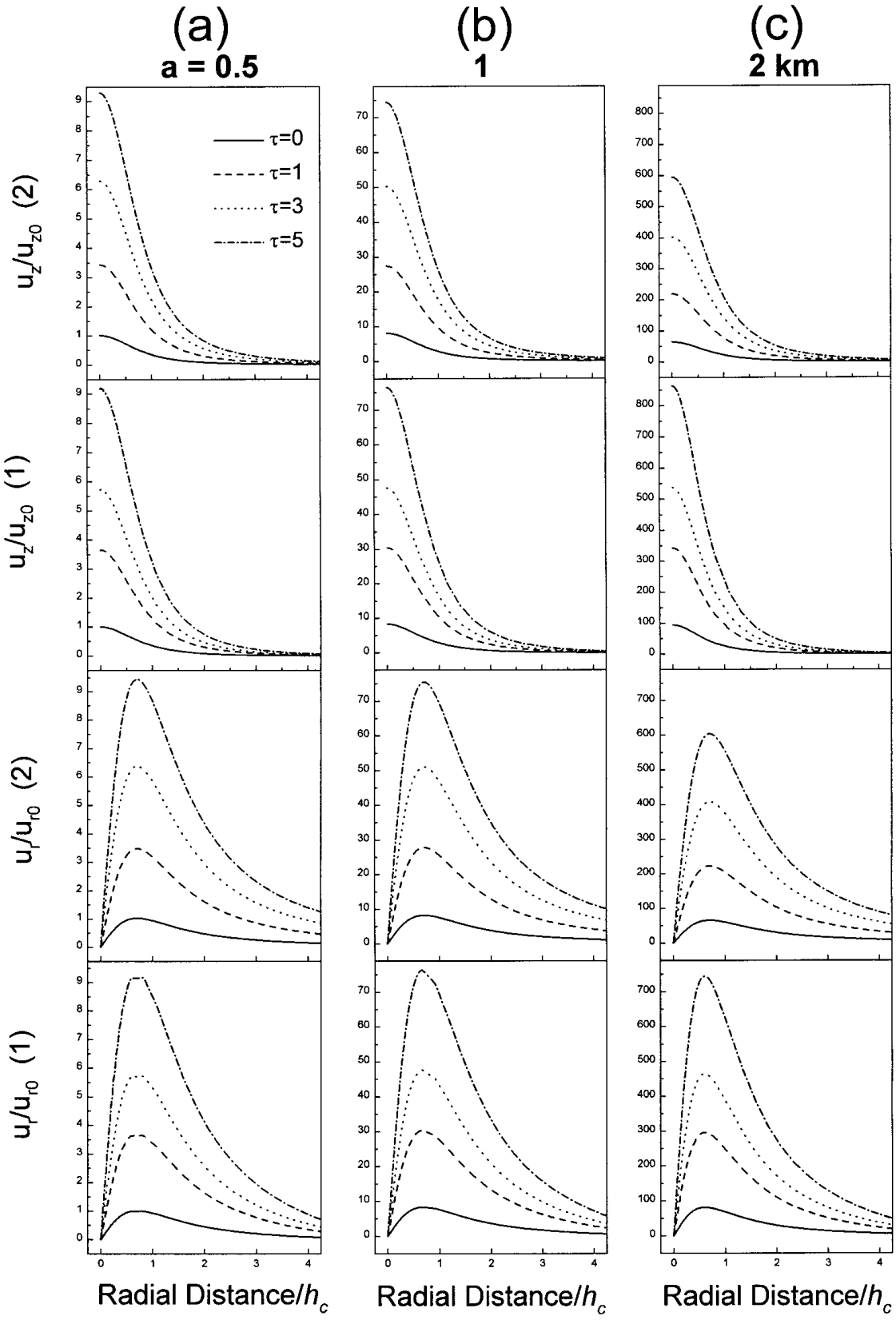

Figure 3. Vertical and radial non-dimensional surface displacements for spherical magma chambers located at 3 km depth with radii of 0.5, 1 and 2 km (Test 1). (1) and (2) indicate numerical results for an extended source and analytical results for a point source, respectively. Vertical, u_z, and radial, u_r, displacements are divided by their respective maxima of elastic displacement (u_{z0} and u_{r0}) for the extended source with radius $a = 0.5$ km. Distances at the surface to the projection of the centre of the magmatic intrusion are also non-dimensional numbers, being radial distance divided by the depth of the source, h_c.

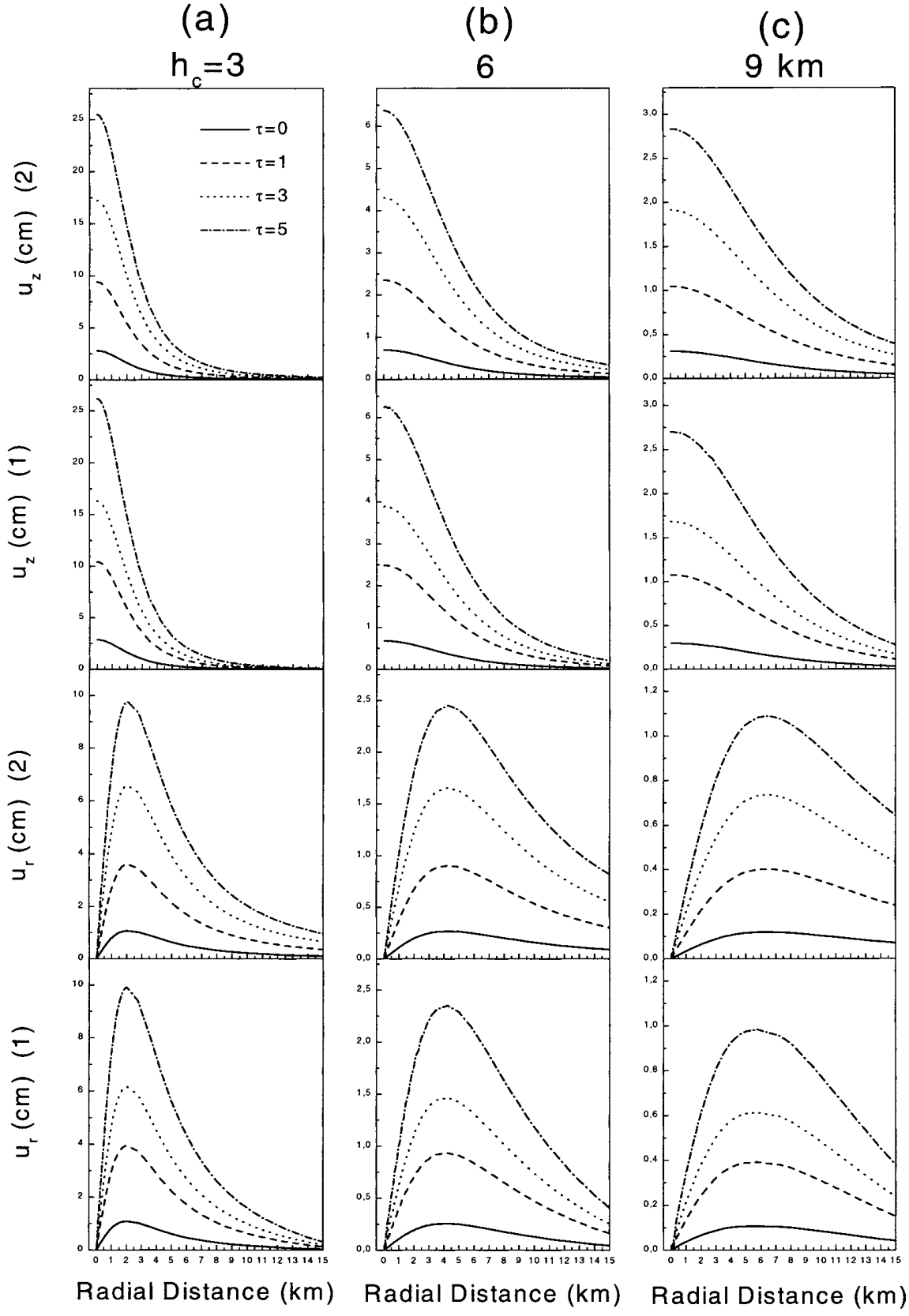

Figure 4. Vertical and radial surface displacements for spherical magma chambers with radii 1 km, located at 3, 6 and 9 km (Test 2).

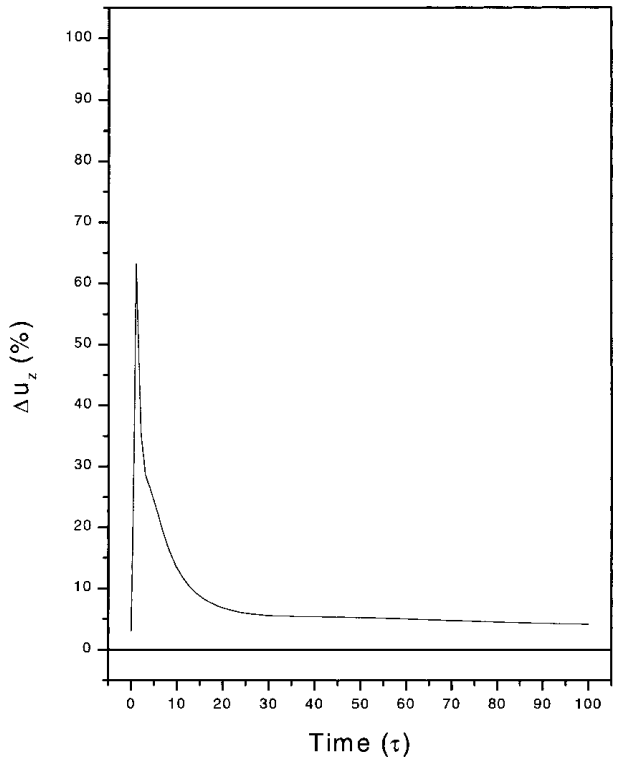

Figure 5. Relative error for vertical displacement $[\Delta u_z = 100(u_z^{\text{num}} - u_z^{\text{ana}})/u_z^{\text{num}}]$ at the point of maximum uplift ($r = 0$) as a function of time. Results for a spherical chamber with $a = 1$ km and $h_c = 3$ km.

substantially a ected by the rheology of the crust. Thus, the main e ect of the type of relaxation is to change the value of the deformation rather than its pattern. However, this e ect is not observed in the case of an elastic layer overlying a lithospheric half-space (see Fig. 7b). In this case, although both solutions coincide at $t = 0$ and at $t = 5\tau$, they are very di erent during other time instants. Thus, the analytical solution (point source) gives a nearly zero viscoelastic displacement, whilst important changes in both magnitude (± 50 per cent of the elastic displacement) and sign are observed in the numerical (extended-source) procedure. It can be an important limitation to the applicability of the point-source hypothesis in the case of such rheological behaviour of the medium. This conclusion is confirmed by the fact that if one considers the same analytical model with no point source (fault plane) and with the same rheological properties, the viscoelastic displacements clearly di er from zero (e.g. Rundle 1982b; Fernández *et al.* 1996, 1998a). Therefore, the rheological properties of the medium and the source type considered (point or extended) are important parameters in interpreting observed time-dependent deformation in active zones.

Finally, Test 6 considers the e ect of the topography assuming axisymmetric volcanoes with average slopes of 15°, 20° and 30°. Both the layer and the half-space are of Relaxation 2 type. Numerical results are compared with the flat-surface solution given by the analytical method without gravitational coupling. The results are shown in Fig. 8. Cayol & Cornet (1998) pointed out that in the elastic case the interpretation of ground-surface displacements with half-space models can lead to erroneous estimations. They found that the steeper the volcano, the flatter the vertical displacement field. This result is dramatically emphasized in the viscoelastic case, where the topography changes both the magnitude and the pattern of the displacement field in a very important way. Thus, for instance, the absolute error between the flat surface and the topographical solutions at $\tau = 5$ can be as high as 350 per cent when $\alpha = 30°$. Neglecting the topographic e ects may, in many cases, introduce an error greater than that implicit in the point-source hypothesis.

4 CONCLUSIONS

Analytical and numerical solutions for ground displacement caused by an overpressurized magma chamber in a layered viscoelastic medium have been obtained considering di erent parameters. Comparison between the two solutions have allowed us to constrain the domain of validity of the point-source and flat-surface hypotheses, which are usually implicitly assumed when deriving analytical solutions. The results obtained show that, as in the elastic case, the greater the value of ε, the greater the discrepancies between the two solutions. Thus, for small ε (radius/depth ratio) values (≤ 0.3) the di erences are in the centimetre range for any time instant. In contrast, for higher ε values the di erences (especially in the vertical direction) can be in the metre range.

With respect to the influence of the shape of the intrusion on the viscoelastic solution, we have compared spherical (point) and ellipsoidal (volumetric) sources. The results obtained show that the eccentricity (e) of the chamber is also an important factor to consider. Very important di erences are found when $e \geq 0.5$. On the other hand, the chamber overpressure does not produce di erences between extended and point sources. As in the elastic case, the vertical displacement produced by a viscoelastic response is proportional to ΔP. In the examples studied we have observed that the main e ect of changing the type of relaxation of the crust is to vary the value of the displacements rather than the deformation pattern. A more detailed study of this e ect was presented by Fernández *et al.* (1998b) and will be described in depth in future work.

The flat-surface hypothesis may, in some cases, introduce an error greater than that implicit in the point source. The e ects of topography on the viscoelastic deformation are qualitatively similar to those produced in the elastic case but the quantitative di erences are dramatically emphasized. Therefore, for an adequate modelling and interpretation of the time-dependent displacements, topography must be considered.

With respect to the inverse problem, we observe that discrepancies between the results obtained for point/volumetric sources are important when we change the size (radius) and shape of the intrusion, as well as the rheology of the inelastic zone. This is not the case when the depth changes. The topography e ect is important but must be studied in depth in connection with the kind of source used in the deformation modelling. The same is true of the e ect of changing the properties of the medium, considering previous results for elastic and elastic gravitational problems (e.g. De Natale & Pingue 1993; Fernández & Rundle 1994; De Natale *et al.* 1997; Fernández *et al.* 1997). A more in-depth study of both e ects will be carried out in future work, including a consideration of the existing gravitational field and the calculation of more e ects of the intrusion in the study (tilt, strain, stress, sea level and gravity changes).

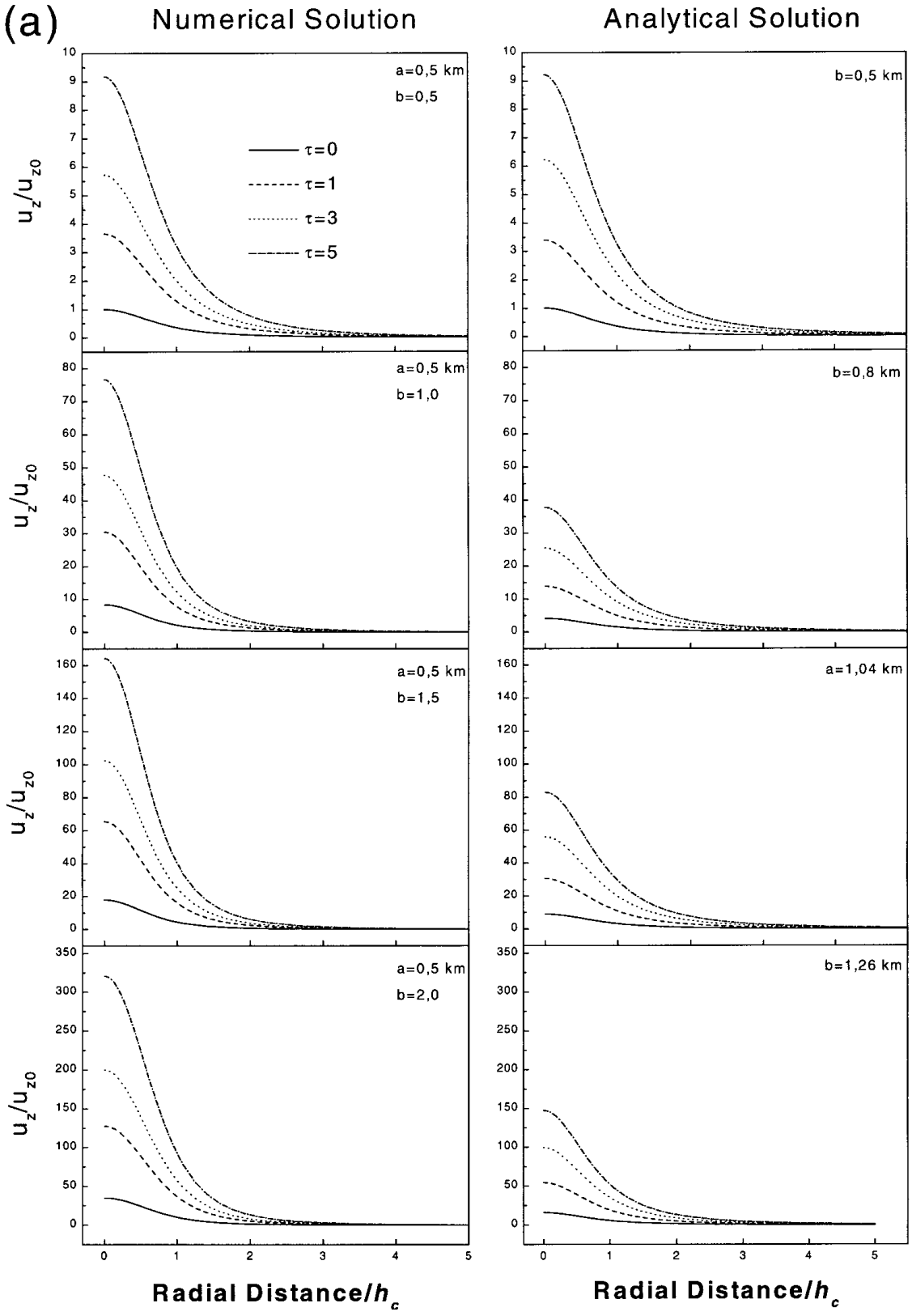

Figure 6. (a) Vertical and (b) radial non-dimensional surface displacements obtained using a numerical model for ellipsoidal chambers with minor axis $b = 0.5$ km and major axis $a = 0.5$, 1, 1.5 and 2 km, the corresponding eccentricities being 0, 0.86, 0.94 and 0.96 respectively. The chamber is at 3 km depth. The same analytical solutions are obtained considering spherical sources with an equal volume (the equivalent radii are 0.5, 0.8, 1.04 and 1.26) (Test 3). Vertical, u_z, and radial, u_r, displacements are divided by their respective maxima of elastic displacement (u_{z0} and u_{r0}) for the extended source with axis $a = b = 0.5$ km. Distances at the surface to the projection of the centre of the magmatic intrusion are also non-dimensional numbers, being the radial distance divided by the depth of the source, h_c.

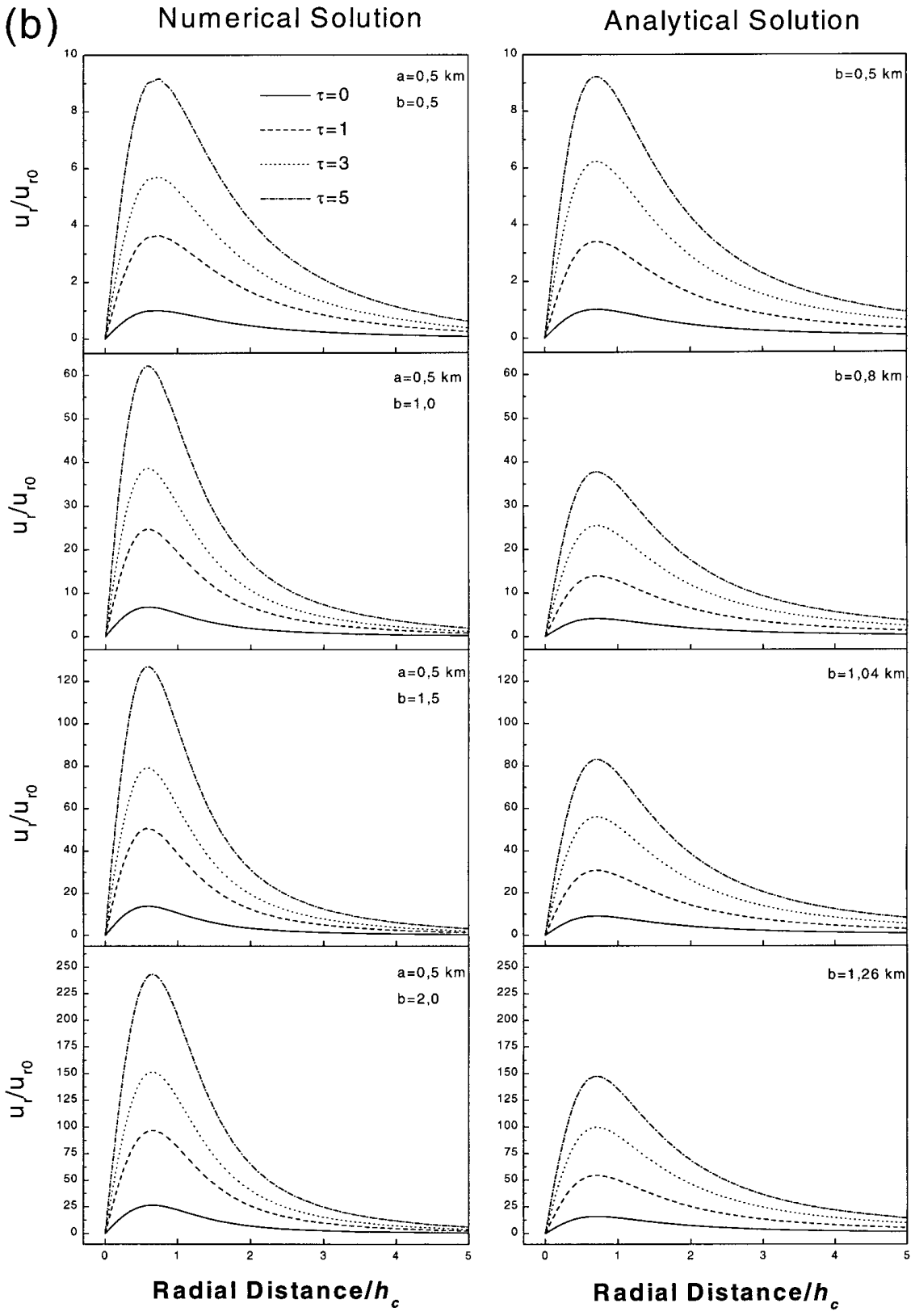

Figure 6. (*Continued.*)

In this work we consider only spherical, and in some cases ellipsoidal, sources and horizontally layered structures, whilst volcanic structures generally have large heterogeneities, as shown by gravity anomalies and seismic topography. Therefore, the models described in this paper are not necessarily applicable, even when the surface pattern of deformation or the Bouguer gravity anomaly is characterized by nearly circular isolines, because these are compatible with any axially symmetric

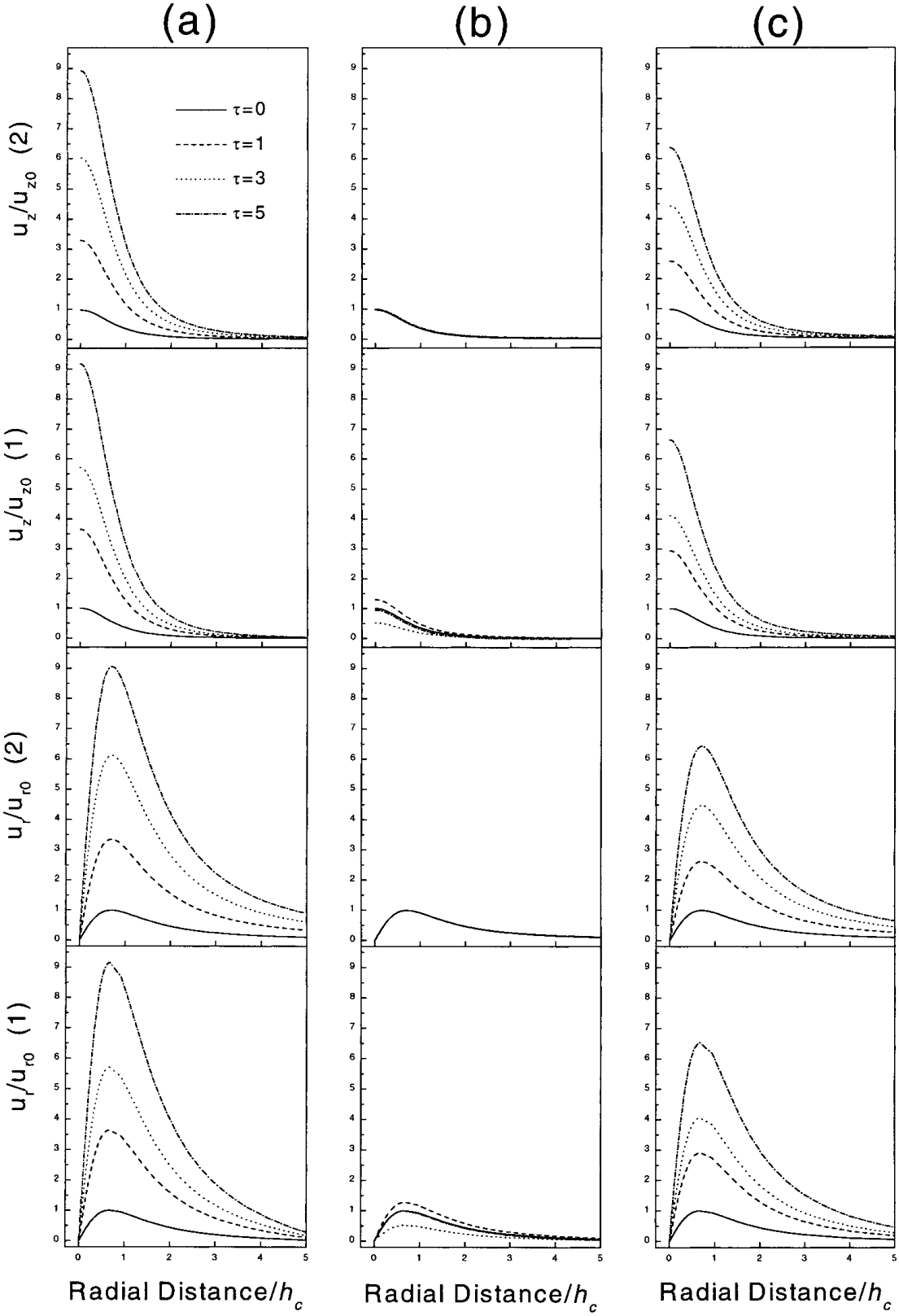

Figure 7. Vertical and radial surface displacements for di erent rheologies in the medium described in Fig. 1. In all cases, $a = b = 1$ km, $h_c = 3$ km, $\Delta P = 10$ MPa, the layer is 10 km thick and no topography is considered (Test 5). Results considering (a) Relaxation 2 for the layer and Relaxation 1 for the bottom half-space, (b) elastic layer and Relaxation 2 for the half-space, and (c) Relaxation 3 and Relaxation 2 for the layer and the half-space respectively. (1) and (2) indicate numerical results for an extended source and analytical results for a point source, respectively. Vertical, u_z, and radial, u_r, displacements are divided by their respective maxima of elastic displacement (u_{z0} and u_{r0}) for the extended source. Distances at the surface to the projection of the centre of the magmatic intrusion are also non-dimensional numbers, being the radial distance divided by the depth of the source, h_c.

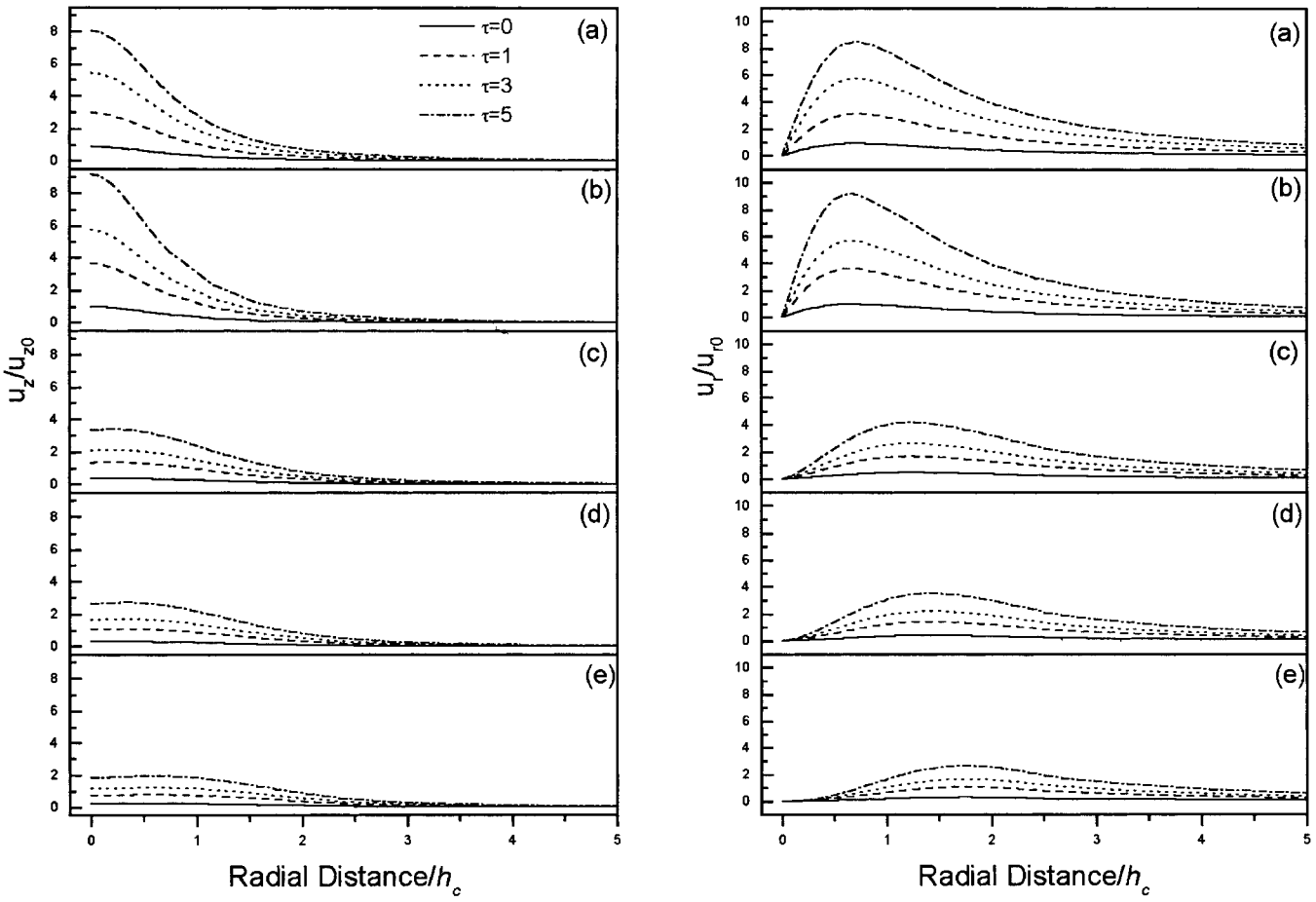

Figure 8. Vertical and radial surface displacements considering topographic e ects (Test 6). (a) Purely viscoelastic analytical solution (flat surface), (b)–(e) purely viscoelastic numerical solutions considering an axisymmetric volcano with an average slope of the flanks of 0°, 15°, 20° and 30°, respectively (the respective heights of the volcano in these cases are 0, 1340, 1820 and 2886 m). Vertical, u_z, and radial, u_r, displacements are divided by their respective maxima of elastic displacement (u_{z0} and u_{r0}) for the extended source and flat surface (b). Distances at the surface to the projection of the centre of the magmatic intrusion are also non-dimensional numbers, being the radial distance divided by the depth of the source, h_c.

structure and source. This paper has mainly investigated the importance of the finite source dimension and topography, but the distortion of actual isolines with respect to the point-source model may be explained by other causes such as axially symmetric buried structures. Also, the seismic activity in the zone must be considered.

ACKNOWLEDGMENTS

This research has been partly founded by the European Commission contract ENV4-CT96–0259 and the CICYT project AMB96–0498-C04. AF is grateful for a CIRIT research fellowship. The research of JBR was supported under US Department of Energy grant number DE-FG03–95ER14499 to the Cooperative Institute for Research in Environmental Sciences (CIRES) at the University of Colorado, Boulder. The research of JF was also partly supported by the contract NASA NAG5–3054 to CIRES at the University of Colorado, Boulder. We also thank M. Bonafede and T. Dahm for reviewing this paper and for their useful comments, which helped to improve it.

REFERENCES

Amelung, F. & Wolf, D., 1994. Viscoelastic perturbations of the earth: significance of the incremental gravitational force in models of glacial isostasy, *Geophys. J. Int.,* **117,** 864–879.

Barker, T.G., 1976. Quasi-static motions near the San Andreas Fault zone, *Geophys. J. Roy. Astrn. Soc.,* **45,** 689–705.

Berrino, G., Corrado, G., Luongo, G. & Toro, B., 1984. Ground deformation and gravity changes accompanying the 1982 Pozzuoli uplift, *Bull. Volc.,* **44,** 187–200.

Berryman, J.G., 1992. E ective stress for transport properties of inhomogeneous porous rock, *J. geophys. Res.,* **97,** 17 409–17 424.

Bianchi, R., Coradini, A., Federico, C., Giberti, G., Lancian, P., Pozzi, J.P., Sartoris, G. & Scandone, R., 1987. Modeling of surface deformation in volcanic area, The 1970–72 1982–84 Crises Campi Flegrei, Italy, *J. geophys. Res.,* **92,** 14 139–14 150.

Bonafede, M., 1990. Axi-symmetric deformation of a thermo-poro-elastic half-space: inflation of a magma chamber, *Geophys. J. Int.,* **103,** 289–299.

Bonafede, M., 1991. Hot fluid migration: an e cient source of ground deformation—Application to the 1982–84 crisis at Phlegrean Fields, Italy, *J. Volc. Geotherm. Res.,* **48,** 187–198.

Bonafede, M., 1995. Interaction between seismic and volcanic deformation: a possible interpretation of ground deformation observed at vulcano Isl (1976–84), *Terra Nova,* **7,** 80–86.

Bonafede, M. & Mazzanti, M., 1998. Modelling gravity variations consistent with ground deformation in the Campi Flegrei caldera (Italy), *J. Volc. Geotherm. Res.,* **81,** 137–157.

Bonafede, M., Dragoni, M. & Quareni, F., 1986. Displacement and stress field produced by a centre of dilatation and by a pressure source in a viscoelastic half-space: application to the study of ground deformation and seismic activity at Campi Flegrei, Italy, *Geophys. J. R. astr. Soc.,* **87,** 455–485.

Cayol, V. & Cornet, F.H., 1998. E ects of topography on the interpretation of the deformation field of prominent volcanoes, Application to Etna, *Geophys. Res. Lett.,* **25,** 1979–1982.

Christensen, R.M., 1971. *Theory of Viscoelasticity, an Introduction,* Academic, New York.

Cost, T.L., 1964. Approximate Lapace transform inversions in viscoelastic stress analysis, *AIAA J.,* **2,** 2157–2166.

Davis, P.M., 1986. Surface deformation due to inflation of an arbitrarily oriented triaxial ellipsoidal cavity in an elastic half-space, with reference to Kilauea volcano, Hawaii, *J. geophys. Res.,* **91,** 7429–7438.

Davis, R.O. & Selvadurai, A.P.S., 1996. *Elasticity and Geomechanics,* Cambridge University Press. Cambridge.

Delaney, P.T. & McTigue, D.F., 1994. Volume of magma accumulation or withdrawal estimated from surface uplift or subsidence, with application to the 1960 collapse of Kilauea volcano, *Bull. Volc.,* **56,** 417–424.

Delaney, P., Denlinger, R., Lisowski, M., Miklius, A., Okubo, P.G., Okamura, T. & Sako, M., 1998. Volcanic spreading at Kilauea, 1976–96, *J. geophys. Res.,* **103,** 18 003–18 023.

De Natale, G. & Pingue, F., 1993. Ground deformations in collapsed caldera structures, *J. Volc. Geotherm. Res.,* **57,** 19–38.

De Natale, G. & Pingue, F., 1996. Ground deformation modeling in volcanic areas, in *Monitoring and Mitigation of Volcano Hazards,* eds Scarpa, R. & Tilling, R.I., pp. 365–388, Springer, Berlin.

De Natale, G., Petrazzuoli, S.M. & Pingue, F., 1997. The e ect of collapse structure on ground deformations in calderas, *Geophys. Res. Lett.,* **24,** 1555–1558.

Deng, J., Gurnis, M., Kanamori, H. & Hauksson, E., 1998. Viscoelastic flow in the lower crust after the 1992 Landers, California, earthquake, *Science,* **282,** 1689–1692.

Dieterich, J.H. & Decker, R.W., 1975. Finite element modeling of surface deformation associated with volcanism, *J. geophys. Res.,* **80,** 4095–4102.

Ding, Z.-Y. & Shen, Y.-Q., 1991. Quasi-static response of a layered viscoelastic half-space to general surface loading, *Phys. Earth planet. Inter.,* **66,** 278–289.

Dragoni, M. & Magnanensi, C., 1989. Displacement and stress produced by a pressurized, spherical magma chamber, surrounded by a viscoelastic shell, *Phys. Earth. planet. Inter.,* **56,** 316–328.

Dvorak, J.J. & Dzurisin, D., 1997. Volcano geodesy: the search for magma reservoirs and the formation of eruptive vents, *Rev. Geophys.,* **35,** 343–384.

Fernández, J. & Rundle, J.B., 1994. Gravity changes and deformation due to a magmatic intrusion in a two-layered crustal model, *J. geophys. Res.,* **99,** 2737–2746.

Fernández, J., Yu, T.T. & Rundle, J.B., 1996. Horizontal viscoelastic-gravitational displacement due to a rectangular dipping thrust fault in a layered Earth model, *J. geophys. Res.,* **101,** 13 581–13 594.

Fernández, J., Rundle, J.B., Granell, R.D.R. & Yu, T.-T., 1997. Programs to compute deformation due to magma intrusion in a elastic-gravitational layered Earth model, *Comput. Geosci.,* **23,** 231–249.

Fernández, J., Yu, T.T. & Rundle, J.B., 1998a. Correction to 'Horizontal viscoelastic-gravitational displacement due to a rectangular dipping thrust fault in a layered Earth model', *J. geophys. Res.,* **103,** 30 283–30 286.

Fernández, J., Tiampo, K., Rundle, J.B., Yu, T.T., Alonso-Medina, A. & Carrasco, J., 1998b. Modelling deformation, potential and gravity changes caused by a magmatic intrusion, *Ann. Geophys.* Suppl. I, **16,** C187.

Fernández, J., Carrasco, J.M., Rundle, J.B. & Araña, V., 1999. Geodetic methods for detecting volcanic unrest, A theoretical approach, *Bull. Volc.,* **60,** 534–544.

Fung, Y.C., 1965. *Foundations of Solid Mechanics,* Prentice Hall, Englewood Cli s, NJ.

Hofton, M.A., Rundle, J.B. & Foulger, G.R., 1995. Horizontal surface deformation due to dike emplacement in an elastic-gravitational layer overlying a viscoelastic-gravitational half-space, *J. geophys. Res.,* **100** (B4), 6329–6338.

Körnig, M. & Müller, G., 1989. Rheological models and interpretation of postglacial uplift, *Geophys. J. Int.,* **98,** 243–253.

Langbein, J., Dzurisin, D., Marshall, G., Stein, R. & Rundle, J.B., 1995. Shallow and peripheral volcanic sources of inflation revealed by modeling two-color geodimeter and leveling data from Long Valley caldera, California, 1988–92, *J. geophys. Res.,* **100,** 12 487–12 495.

Mavko, G. & Nur, A., 1975. Melt squirt in the asthenosphere, *J. geophys. Res.,* **80,** 1444–1448.

McTigue, D.F., 1987. Elastic stress and deformation near a finite spherical magma body: resolution of the point source paradox, *J. geophys. Res.,* **92,** 12 931–12 940.

McTigue, D.F. & Segall, P., 1988. Displacements and tilts from dip-slip faults and magma chambers beneath irregular surface topography, *Geophys. Res. Lett.,* **15,** 601–604.

McTigue, D.F. & Stein, R.S., 1984. Topographic amplification of tectonic displacement: implications for geodetic measurement of strain changes, *J. geophys. Res.,* **89,** 1123–1131.

Melosh, H.J., 1976. Nonlinear stress propagation in the earth's upper mantle, *J. geophys. Res.,* **81,** 5621–5632.

Melosh, H.J. & Raefsky, A., 1983. Anelastic response of the Earth to a dip slip earthquake, *J. geophys. Res.,* **88,** 515–526.

Mogi, K., 1958. Relations of the eruptions of various volcanoes and the deformations of the ground surface around them, *Bull. Earthq. Res. Inst., University of Tokyo,* **36,** 99–134.

Nur, A. & Mavko, G., 1974. Post-seismic viscoelastic rebound, *Science,* **183,** 204–206.

Peltier, W.R., 1974. The impulse response of a Maxwell earth, *Rev. Geophys. Space Phys.,* **12,** 649–669.

Peltier, W.R., 1982. Dynamics of the ice-age Earth, *Adv. Geophys.,* **24,** 1–146.

Peltier, W.R., 1998. Postglacial variations in the level of the sea: implications for climate dynamics and solid-Earth geophysics, *Rev. Geophys.,* **36,** 603–689.

Pollitz, F.F., 1997. Gravitational viscoelastic postseismic relaxation on a layered spherical Earth, *J. geophys. Res.,* **102,** 17 921–17 941.

Rundle, J.B., 1976. Anelastic processes in strike slip faulting: Application to the San Francisco earthquake of 1906, *PhD Dissertation,* University of California at Los Angeles, Los Angeles.

Rundle, J.B., 1978. Viscoelastic crustal deformation by finite quasi-static sources, *J. geophys. Res.,* **83,** 5937–5945.

Rundle, J.B., 1980. Static elastic-gravitational deformation of a layered half space by point couple sources, *J. geophys. Res.,* **85,** 5355–5363.

Rundle, J.B., 1981. Numerical evaluation of static elastic-gravitational deformation in a layered half space by point couple sources, *Sandia Rept.,* **81,** 2058.

Rundle, J.B., 1982a. Deformation, gravity, and potential changes due to volcanic loading of the crust, *J. geophys. Res.,* **87,** 10 729–10 744.

Rundle, J.B., 1982b. Viscoelastic-gravitational deformation by a rectangular thrust fault in a layered Earth, *J. geophys. Res.,* **87,** 7787–7796.

Rundle, J.B., 1982c. Some solutions for static and pseudo-static deformation in layered, nonisothermal, porous media, *J. Phys. Earth,* **30,** 421–440.

Rundle, J.B., 1983. Correction to 'The deformation, gravity, and potential changes due to volcanic loading of the crust', *J. geophys. Res.,* **88,** 10 647–10 653.

Rundle, J.B. & Jackson, D.D., 1977a. A viscoelastic relaxation model for postseismic deformation from the San Francisco earthquake of 1906, *Pure appl. Geophys.,* **115,** 401–411.

Rundle, J.B. & Jackson, D.D., 1977b. A three-dimensional viscoelastic model of a strike-slip fault, *Geophys. J. R. astr. Soc.,* **49,** 575–591.

Rundle, J.B. & Jackson, D.D., 1977c. A kinematic viscoelastic model of the San Francisco earthquake of 1906, *Geophys. J. R. astr. Soc.,* **50,** 441–458.

Rymer, H., 1996. Microgravity monitoring, in *Monitoring and Mitigation of Volcano Hazards,* pp. 169–197, eds Scarpa, R. & Tilling, R.I., Springer, Berlin.

Rymer, H., Cassidy, J., Locke, C.A. & Murray, J.B., 1995. Magma movements in Etna volcano associated with the major 1991–93 lava eruption: evidence from gravity and deformation, *Bull. Volc.,* **57,** 451–461.

Sartoris, G., Pozzi, J.P., Philippe, C. & Moüel, J.L., 1990. Mechanical stability of shallow magma chambers, *J. geophys. Res.,* **95,** 5141–5151.

Schapery, R.A., 1961. Approximate methods of transform inversion for viscoelastic stress analysis, *Proc. 4th US Nat. Congr. appl. Mech,* **2,** 1075–1085.

Tilling, R.I. & Dvorak, J.J., 1993. Anatomy of a basaltic volcano, *Nature,* **363,** 125–133.

Vermeersen, L.L.A., Sabadini, R. & Spada, G., 1996. Analytical visco-elastic relaxation models, *Geophys. Res. Lett.,* **23,** 697–700.

Williams, C.A. & Wadge, G., 1998. The e ects of topography on magma chamber deformation models: applications to Mt Etna and radar interferometry, *Geophys. Res. Lett.,* **25,** 1549–1552.

Wolf, D., 1984. The relaxation of spherical and flat Maxwell Earth models and e ects due to the presence of the lithosphere, *J. Geophys.,* **56,** 24–33.

Yu, T.-T., Rundle, J.B. & Fernández, J., 1996. Surface deformation due to strike slip fault in an elastic gravitational layer overlying a viscoelastic gravitational half space, *J. geophys. Res.,* **101,** 3199–3214.

Yu, T.-T., Rundle, J.B. & Fernández, J., 1999. Correction to 'Surface deformation due to strike slip fault in an elastic gravitational layer overlying a viscoelastic gravitational half space', *J. geophys. Res.,* **104,** 15 313–15 316.